

## Supporting Information

# Systematic Study on Swelling/Delamination of Layered Metal Oxides with Quaternary Ammonium Ions: Production of Well-Shaped/Oversized Unilamellar Nanosheets

*Yeji Song,<sup>a,b</sup> Nobuyuki Sakai,<sup>a</sup> Yasuo Ebina,<sup>a</sup> Nobuo Iyi,<sup>a</sup> Takayuki Kikuchi, Renzhi Ma,<sup>a</sup> Yasuhiro Ishida,<sup>c</sup> and Takayoshi Sasaki<sup>\*a,b</sup>*

<sup>a</sup> Research Center for Materials Nanoarchitectonics (MANA), National Institute for Materials Science (NIMS), 1-1 Namiki, Tsukuba, Ibaraki 305-0044, Japan.

<sup>b</sup> Materials Science and Engineering, Graduate School of Pure and Applied Sciences, University of Tsukuba, 1-1-1 Tennodai, Tsukuba, Ibaraki 305-8577, Japan.

<sup>c</sup> RIKEN Center for Emergent Matter Science, 2-1 Hirosawa, Wako, Saitama 351-0198, Japan.

\*Corresponding author. E-mail: SASAKI.Takayoshi@nims.go.jp

## S1. Experimental Section

### Synthesis of Platelet Crystals of Layered Perovskite and Titanate.

Platelet single crystals of  $\text{KCa}_2\text{Nb}_3\text{O}_{10}$  were synthesized via the  $\text{K}_2\text{SO}_4$  flux-mediated growth method. Briefly, a mixture of  $\text{K}_2\text{SO}_4$ ,  $\text{CaCO}_3$ , and  $\text{Nb}_2\text{O}_5$  (5:4:3 in molar ratio) was heated at 1300 °C for 24 h and then cooled to 800 °C at a rate of 25 °C h<sup>-1</sup>. Subsequently, the sample was naturally cooled down to room temperature, and the crystals were collected by dissolving away the flux with water and drying under vacuum. The crystal size in the range of 25–53 μm was classified by sieving to collect samples suitable for swelling/exfoliation experiments in this study (Figure S3). A weighed amount (2.0 g) of  $\text{KCa}_2\text{Nb}_3\text{O}_{10}$  crystals was treated with 80 cm<sup>3</sup> of a 5 M  $\text{HNO}_3$  aqueous solution at ambient temperature for 6 days to convert the crystals into the protonated form,  $\text{HCa}_2\text{Nb}_3\text{O}_{10} \cdot 1.5\text{H}_2\text{O}$ . The acid solution was replaced with a fresh one three times. The final product was recovered through filtration, rinsing with a copious quantity of water, and then air-dried. XRD profiles of the obtained crystals, both potassium and protonated forms (Figure S2), agree well with previous studies.<sup>[28,29]</sup>

Platelet crystals of the lepidocrocite-type titanate,  $\text{K}_{0.8}\text{Ti}_{1.73}\text{Li}_{0.27}\text{O}_4$ , were synthesized

according to a modified process for the isomorphous compound of  $K_{0.8}Ti_{1.2}Fe_{0.8}O_4$ .<sup>[26,27]</sup> A flux melt of  $K_2MoO_4$  containing a stoichiometric mixture of  $K_2CO_3/Li_2CO_3/TiO_2$  was heated at 1120 °C for 20 h and then cooled to room temperature. The obtained crystals were collected and converted into the acid-exchanged form of  $H_{1.07}Ti_{1.73}O_4 \cdot H_2O$ .

### **Equilibration for Swelling and Exfoliation.**

A weighed amount (0.2 g) of  $HCa_2Nb_3O_{10} \cdot 1.5H_2O$  was gently mixed with 100 cm<sup>3</sup> of four TAAOH aqueous solutions. The concentration of TAAOH was fixed at 3.657 mM, corresponding to the equivalent molar ratio of TAA to the cation exchange capacity of  $HCa_2Nb_3O_{10} \cdot 1.5H_2O$ . TMAOH (15% in H<sub>2</sub>O, FUJIFILM Wako Chemicals), TEAOH (20% in H<sub>2</sub>O, FUJIFILM Wako Chemicals), TPAOH (20–25% in H<sub>2</sub>O, Tokyo Chemical Industry), and TBAOH (10% in H<sub>2</sub>O, FUJIFILM Wako Chemicals) were used as received to prepare the solutions at this concentration. The reaction mixtures were kept still overnight to achieve equilibration and to settle the swollen product on the bottom of the reaction flask. To facilitate exfoliation, the solution with the swollen crystals was agitated by a reciprocal mechanical shaker at 160 rpm for 24 h. After shaking, specimens were centrifuged at 1500 rpm for 10 min to separate unilamellar nanosheets (top suspension) from unexfoliated crystal residues (sediment). Equilibration of  $H_{1.07}Ti_{1.73}O_4 \cdot H_2O$  with TAA solutions was conducted similarly to the procedure above for  $HCa_2Nb_3O_{10} \cdot 1.5H_2O$ .

The amount of intercalated TAA ions was estimated via acid-base titration by determining the solution concentration before and after equilibration. The aliquot (20 cm<sup>3</sup>) of supernatants was taken out from the mixture and subjected to titration with a standard HCl solution. The change in pH was recorded with a pH meter to obtain the point of neutralization.

### **Determination of the Exfoliation Yield.**

The exfoliation yield was estimated based on UV-vis absorption spectra and molar extinction coefficient of the  $Ca_2Nb_3O_{10}^-$  nanosheet suspensions based on the Lambert-Beer law. The molar extinction coefficient ( $\epsilon$ ) was determined by the combination of gravimetric quantification of the solid content upon heating at 1000 °C and spectroscopic analysis. First, the nanosheet suspension was centrifuged at 1500 rpm (420 g) to remove the unexfoliated portion. A certain volume (2 cm<sup>3</sup>) of the suspension was loaded in a Pt crucible and the water was slowly evaporated at 60 °C. A dried residue of nanosheets with  $TBA^+$  ions was calcined at 1000 °C for 6 h to produce an oxide sample in a nominal composition of  $Ca_2Nb_3O_{9.5}$ . The average weight of 3 specimens was 3.55 mg of  $Ca_2Nb_3O_{9.5}$  in 2 cm<sup>3</sup>, corresponding to 3.474 mmol dm<sup>-3</sup> of  $Ca_2Nb_3O_{10}^-$  nanosheets. For the spectroscopic analysis, the nanosheet suspension was diluted 100 times to obtain a suitable magnitude of absorbance, 0.8555 at 265 nm. Based on the above results, the molar extinction coefficient of the  $Ca_2Nb_3O_{10}^-$  nanosheets was calculated as  $\epsilon = 2.46 \times 10^4 \text{ mol}^{-1} \text{ dm}^3 \text{ cm}^{-1}$  at 265

nm. This value was used to calculate the exfoliation yield of the specimen.

### **Deposition of Nanosheets for Observations by AFM.**

A Si wafer substrate was cleaned by immersing it in methanol/HCl (1:1 in volume) and subsequently in concentrated H<sub>2</sub>SO<sub>4</sub> for 30 min each. After rinsing thoroughly, the substrate was immersed in an aqueous solution of polyethylenimine (PEI, 1.25 g dm<sup>-3</sup>, and pH = 9) to introduce a positive charge of the surface. Afterwards, the PEI primed Si substrate was dipped into the suspension of nanosheets for 15 min and washed with pure water to eliminate excess nanosheets on the surface. AFM observation was conducted on the resulting samples.

### **Sample Characterization.**

XRD data were recorded using Rigaku ULTIMA IV powder diffractometer with a graphite monochromatized Cu K $\alpha$  radiation ( $\lambda = 0.15405$  nm). The swollen crystals equilibrated with TAAOH solutions were examined by SAXS technique using Rigaku NANO-viewer with Cu K $\alpha$  radiation. A few drops of samples were packed in a sample holder with a hollow slit using Scotch tape. Three scan data (30 min each) were collected for each sample and averaged. Polarized optical microscopy images of the swollen crystals were recorded with an Olympus BX51 optical microscope. AFM images of the nanosheets deposited on a Si substrate were measured with the instrument (SPI3800N/SPA-400, Hitachi High-Tech Corporation) employing a Si cantilever (20 N m<sup>-1</sup>) with noncontact mode. The lateral size of nanosheets was statistically analyzed based on several AFM and scanning electron microscopy (SEM; JSM-6010LA, JEOL) images. An adequate number, 106 to 128 sheets per specimen, was measured. Image processing was performed using ImageJ software to distinguish the area of individual nanosheets. Then, the average size of nanosheets was expressed as a diameter by approximating their shape as circles, ignoring the varied shapes of the nanosheets. UV-vis absorption spectra of the suspensions were recorded with a spectrophotometer (U-4100, Hitachi). FT-IR spectra of the restacked nanosheets were collected on Perkin-Elmer Spectrum One using universal attenuated total reflection (ATR) sampling accessory.

## S2. Supporting Figures and Tables

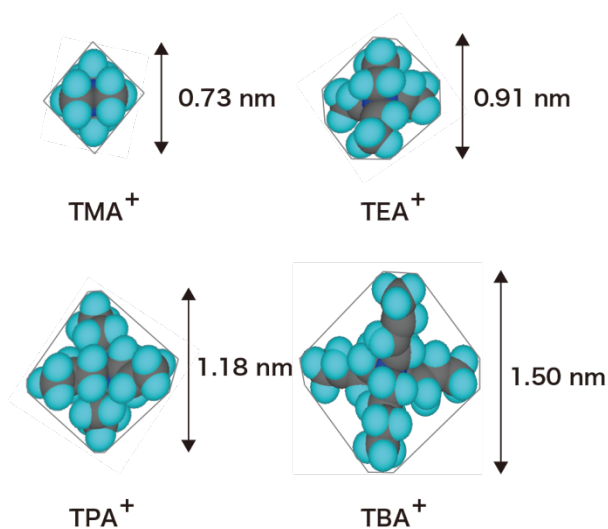


**Figure S1.** Molecular structures of TAA ions viewed along the  $C_2$  axis. Blue and gray balls represent hydrogen and carbon atoms, respectively. The alkyl chain length, denoted as  $n$ , is characterized as  $n = 1, 2, 3$ , and  $4$  for TMA, TEA, TPA, and TBA ions, respectively.

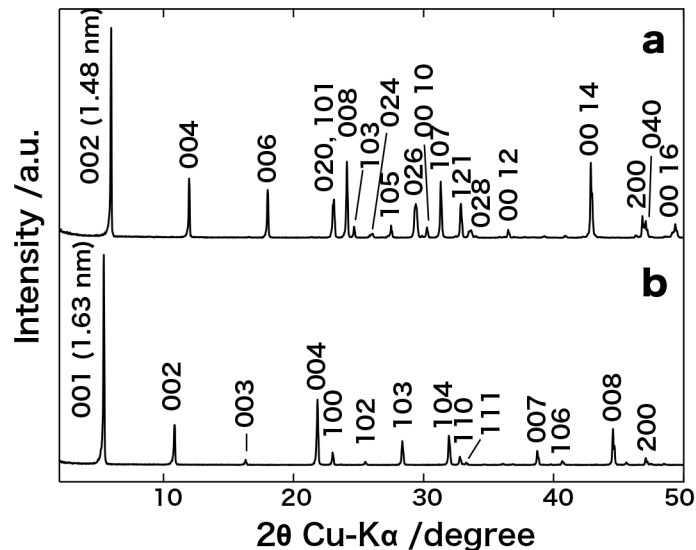


**Figure S2.** XRD patterns of a)  $KCa_2Nb_3O_{10}$  and b)  $HCa_2Nb_3O_{10} \cdot 1.5H_2O$ . All peaks can be indexed in terms of orthorhombic [ $a = 0.3875(1)$  nm,  $b = 0.7709(3)$  nm,  $c = 2.9486(8)$  nm] and tetragonal [ $a = 0.3855(1)$  nm,  $c = 1.6225(2)$  nm] unit cells for  $KCa_2Nb_3O_{10}$  and  $HCa_2Nb_3O_{10} \cdot 1.5H_2O$ , respectively.

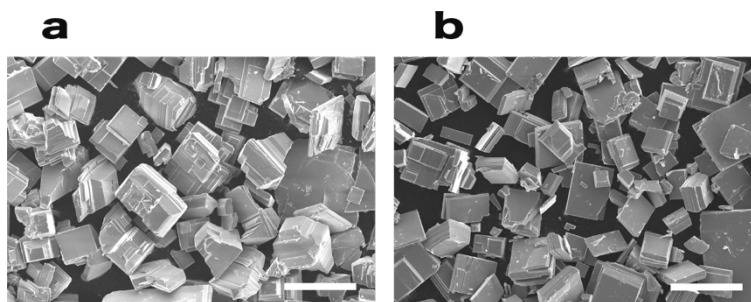


**Figure S3.** SEM images of a)  $\text{KCa}_2\text{Nb}_3\text{O}_{10}$  and b)  $\text{HCa}_2\text{Nb}_3\text{O}_{10} \cdot 1.5\text{H}_2\text{O}$ . No apparent morphological change was observed after the treatment. The scale bars represent  $50 \mu\text{m}$ .

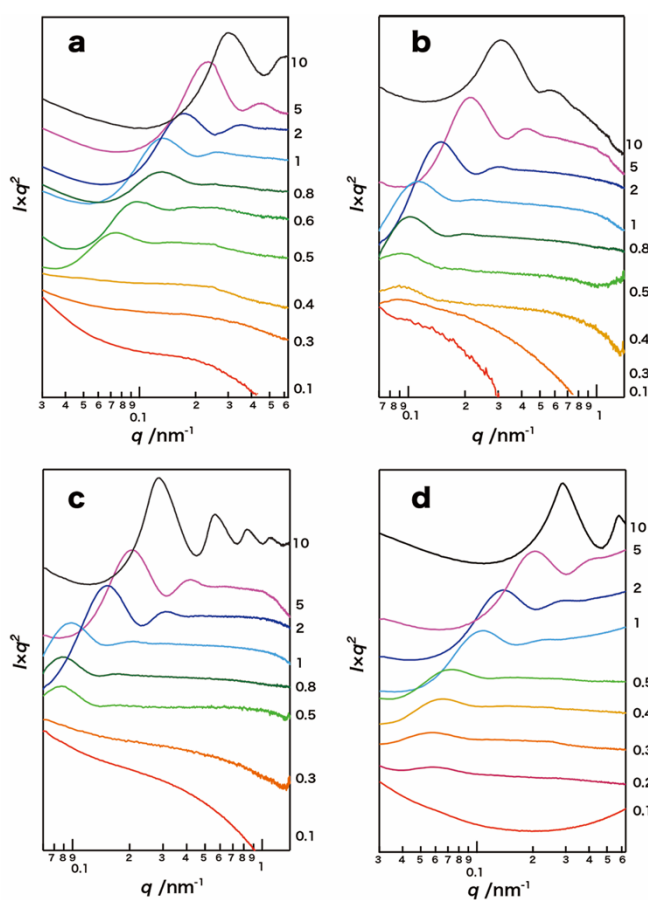


**Figure S4.** SAXS profiles of swollen crystals of  $\text{HCa}_2\text{Nb}_3\text{O}_{10} \cdot 1.5\text{H}_2\text{O}$  in a) TMAOH, b) TEAOH, c) TPAOH, and d) TBAOH solutions at various concentrations. Values of  $I \times q^2$  are plotted as a function of the scattering vector,  $q$ , where  $I$  represents the scattering intensity. The numbers next to the profiles indicate the concentrations of the solutions in terms of  $\text{TAA}^+/\text{H}^+$ .

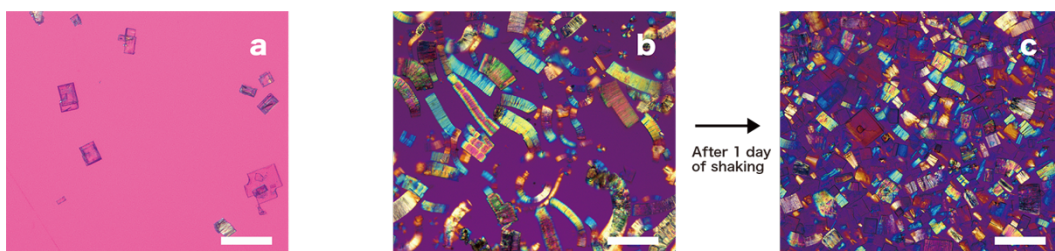


**Figure S5.** Polarized optical microscope images of a) the pristine crystals of  $\text{HCa}_2\text{Nb}_3\text{O}_{10} \cdot 1.5\text{H}_2\text{O}$  and the swollen ones with the TMAOH solution b) before and c) after 1 day of shaking. The scale bars indicate 100  $\mu\text{m}$ .

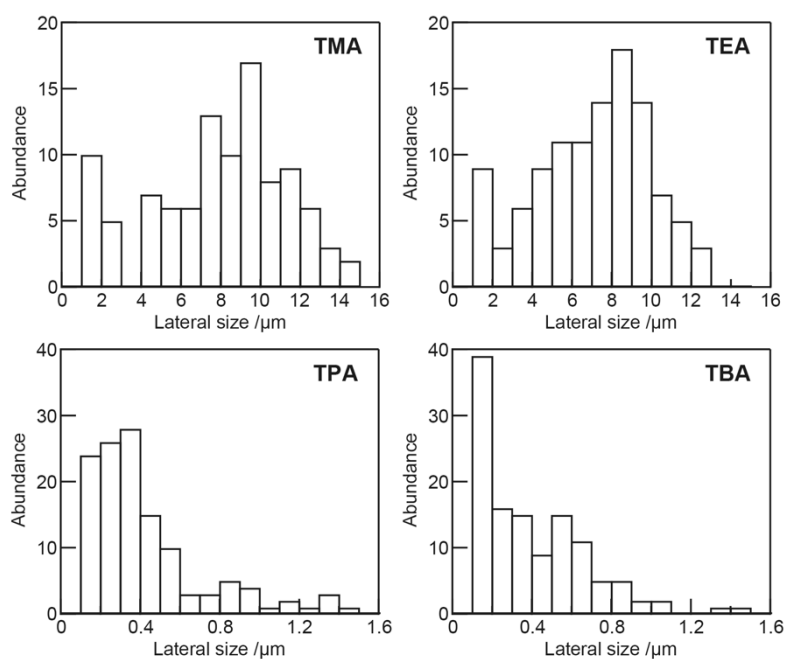


**Figure S6.** Size distributions of  $\text{Ca}_2\text{Nb}_3\text{O}_{10}^-$  nanosheets obtained in TAAOH solutions.

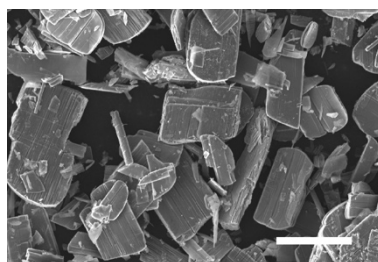


**Figure S7.** SEM images of the lepidocrocite-type layered titanate crystals of  $\text{H}_{1.07}\text{Ti}_{1.73}\text{O}_4 \cdot \text{H}_2\text{O}$ . The scale bars represent 50  $\mu\text{m}$ .

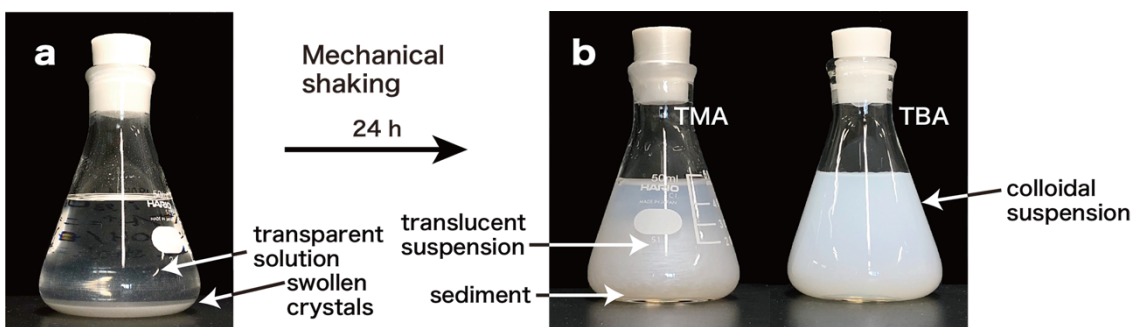


**Figure S8.** Photographs of a) swollen crystals of  $\text{H}_{1.07}\text{Ti}_{1.73}\text{O}_4 \cdot \text{H}_2\text{O}$  equilibrated with TAA solutions and b) samples after mechanical shaking.

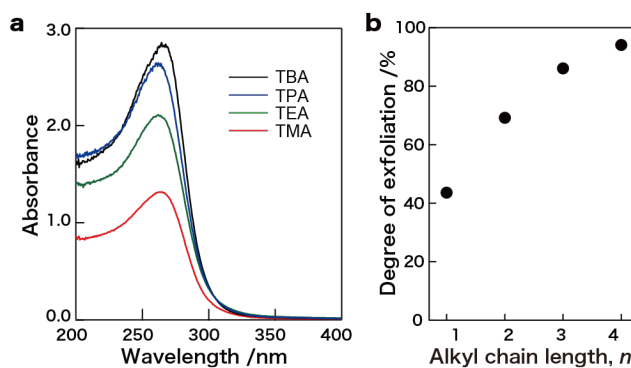


**Figure S9.** a) UV-vis absorption spectra of  $\text{Ti}_{0.87}\text{O}_2^{0.52-}$  nanosheet suspensions, diluted 100 times with water. b) The exfoliation yields calculated from the absorbance at 266 nm.

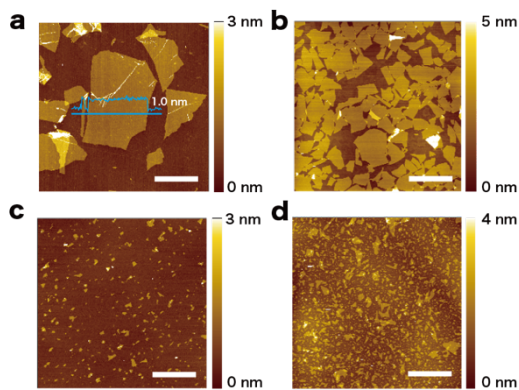


**Figure S10.** AFM images of  $\text{Ti}_{0.87}\text{O}_2^{0.52-}$  nanosheets obtained in a) TMAOH, b) TEAOH, c) TPAOH, and d) TBAOH solutions. The scale bars represent 5  $\mu\text{m}$ .

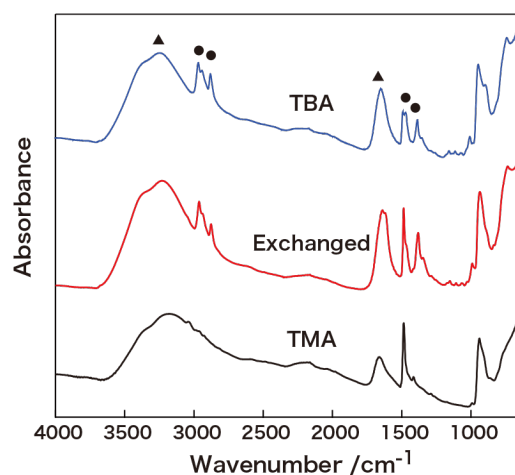


**Figure S11.** FT-IR spectra of the restacked flakes of  $\text{Ca}_2\text{Nb}_3\text{O}_{10}^-$  nanosheets obtained in TBAOH, TMAOH, and after exchange from TMAOH to TBAOH solutions. The absorption bands indicated by circles, observed in a range of  $3000\text{--}2800\text{ cm}^{-1}$  and  $1500\text{--}1300\text{ cm}^{-1}$ , are attributed to stretching and deformation of  $-\text{CH}_2-$  and  $-\text{CH}_3$  groups, respectively. The broad band in a range of  $3600\text{--}2800\text{ cm}^{-1}$  and the band at  $1630\text{ cm}^{-1}$ , labelled by triangles, are assigned as stretching and bending modes of  $-\text{OH}$  and  $\text{H}_2\text{O}$ , respectively.

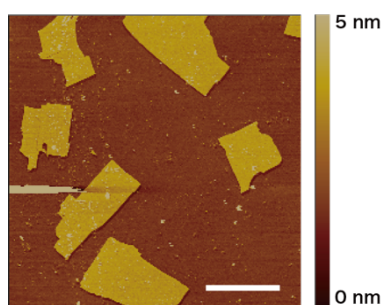


**Figure S12.** AFM images of  $\text{Ca}_2\text{Nb}_3\text{O}_{10}^-$  nanosheets obtained via exfoliation in the TMAOH solution, followed by sedimentation upon centrifugation at 10000 rpm for 30 min and redispersion into the equal volume of TMAOH solution. The scale bar represents  $5\text{ }\mu\text{m}$ .

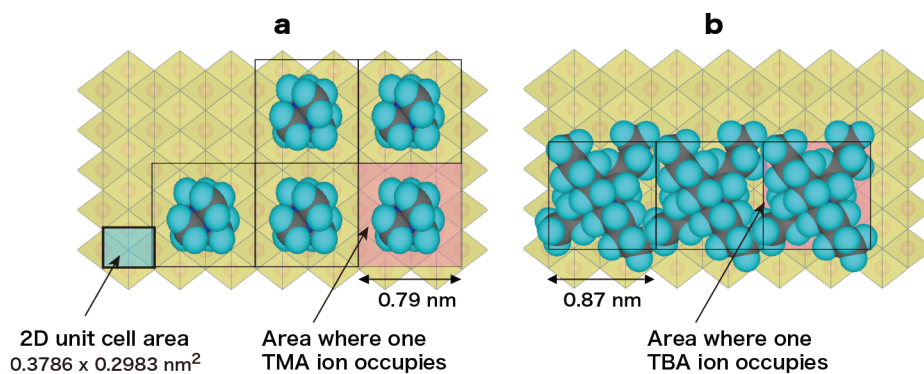


**Figure S13.** Schematic illustrations of adsorbed a) TMA and b) TBA ions on the host layer of  $\text{Ti}_{0.87}\text{O}_2^{0.52-}$ . TMA ions are isolated from neighboring ions, while TBA ions are in contact to each other.

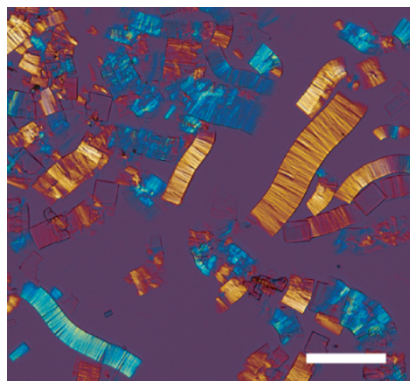


**Figure S14.** Polarized optical microscopy image of swollen crystals of  $\text{HCa}_2\text{Nb}_3\text{O}_{10} \cdot 1.5\text{H}_2\text{O}$  with TBA ions after solvent exchange to DMSO. Scale bar indicates 100  $\mu\text{m}$ .

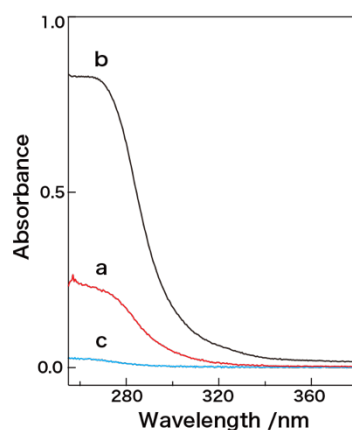


**Figure S15.** a) UV-vis absorption spectra of colloidal suspensions of  $\text{Ca}_2\text{Nb}_3\text{O}_{10}^-$  nanosheets exfoliated from swollen crystals with TBA ions in DMSO via mechanical shaking. Those b) from swollen crystals with TBA ions in  $\text{H}_2\text{O}$  and c) from swollen crystals with TMA ions in  $\text{H}_2\text{O}$ , respectively.

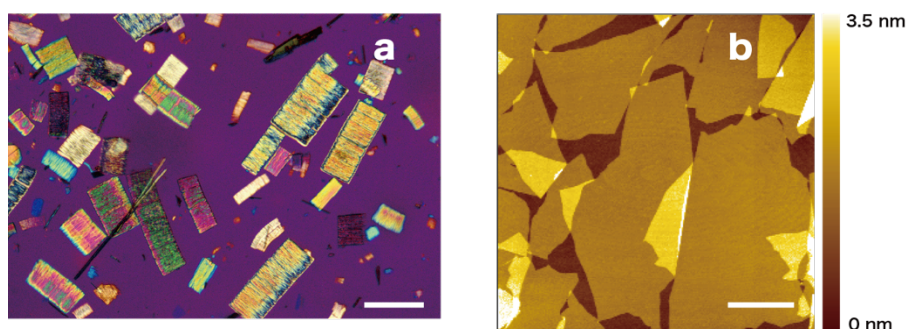


**Figure S16.** a) Polarized optical microscopy image of swollen crystals of  $\text{H}_{1.07}\text{Ti}_{1.73}\text{O}_4 \cdot \text{H}_2\text{O}$  with TBA ions after solvent exchange to DMSO. The scale bar indicates  $100 \mu\text{m}$ . b) AFM image of  $\text{Ti}_{0.87}\text{O}_2^{0.52-}$  nanosheets exfoliated from swollen titanate crystals via mechanical shaking in DMSO. The scale bar represents  $2 \mu\text{m}$ .

**Table S1.** Comparison of the area occupied by one TAA ion on the  $\text{Ca}_2\text{Nb}_3\text{O}_{10}^-$  nanosheets and its projected area.

	TMA	TEA	TPA	TBA
Uptake	59%	51%	44%	37%
Area occupied by one TAA ion	$0.504 \text{ nm}^2$	$0.583 \text{ nm}^2$	$0.676 \text{ nm}^2$	$0.803 \text{ nm}^2$
Projected area of TAA ion	$0.271 \text{ nm}^2$	$0.413 \text{ nm}^2$	$0.698 \text{ nm}^2$	$1.122 \text{ nm}^2$